Cell Reports, Volume *25*

Supplemental Information

Blimp-1 Functions as a Molecular Switch to Prevent Inflammatory Activity in Foxp3^{+}RORγt^{+} Regulatory T Cells

Chihiro Ogawa, Rashmi Bankoti, Truc Nguyen, Nargess Hassanzadeh-Kiabi, Samantha Nadeau, Rebecca A. Porritt, Michael Couse, Xuemo Fan, Deepti Dhall, Gerald Eberl, Caspar Ohnmacht, and Gislâine A. Martins

Supplemental Figure 1

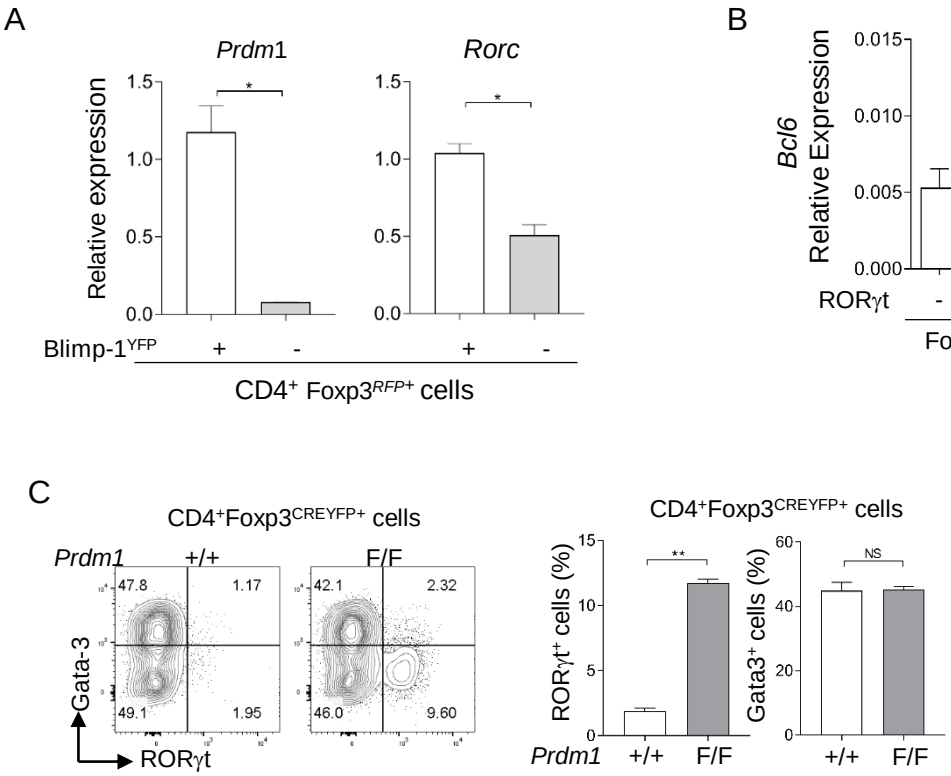

Supplemental Figure 1: Blimp-1 expression in RORγt$^+$Foxp3$^+$Treg cells, related to Figure 1. (**A**) *Prdm1* and *Rorc* mRNA expression (qRT-PCR, relative to β2microglobulin) in CD4$^+$Foxp3^{RFP+}Blimp-1^{YFP-} and CD4$^+$Foxp3^{RFP+}Blimp-1^{YFP+} cells sorted from Blimp-1^{YFP}Foxp3^{RFP} dual reporter mice. **(B**) *Bcl6* mRNA expression (qRT-PCR) in same cells shown in Fig. 1B. (**C**) Frequency of RORγt$^+$ and GATA-3$^+$ cells in CD4$^+$Foxp3$^{CREYFP+}$ cells from the mesenteric lymph nodes from *Prdm1*$^{+/+}$Foxp3$^{CREYFP+}$ or *Prdm1*$^{F/F}$Foxp3$^{CREYFP+}$ mice. Data shown is from at least two independent experiments. Bars show average and error bars, SEM (N ≧ 3 mice/group). **p*<0.05 and ***p*<0.01, unpaired student's *t* test.

Supplemental Figure 2

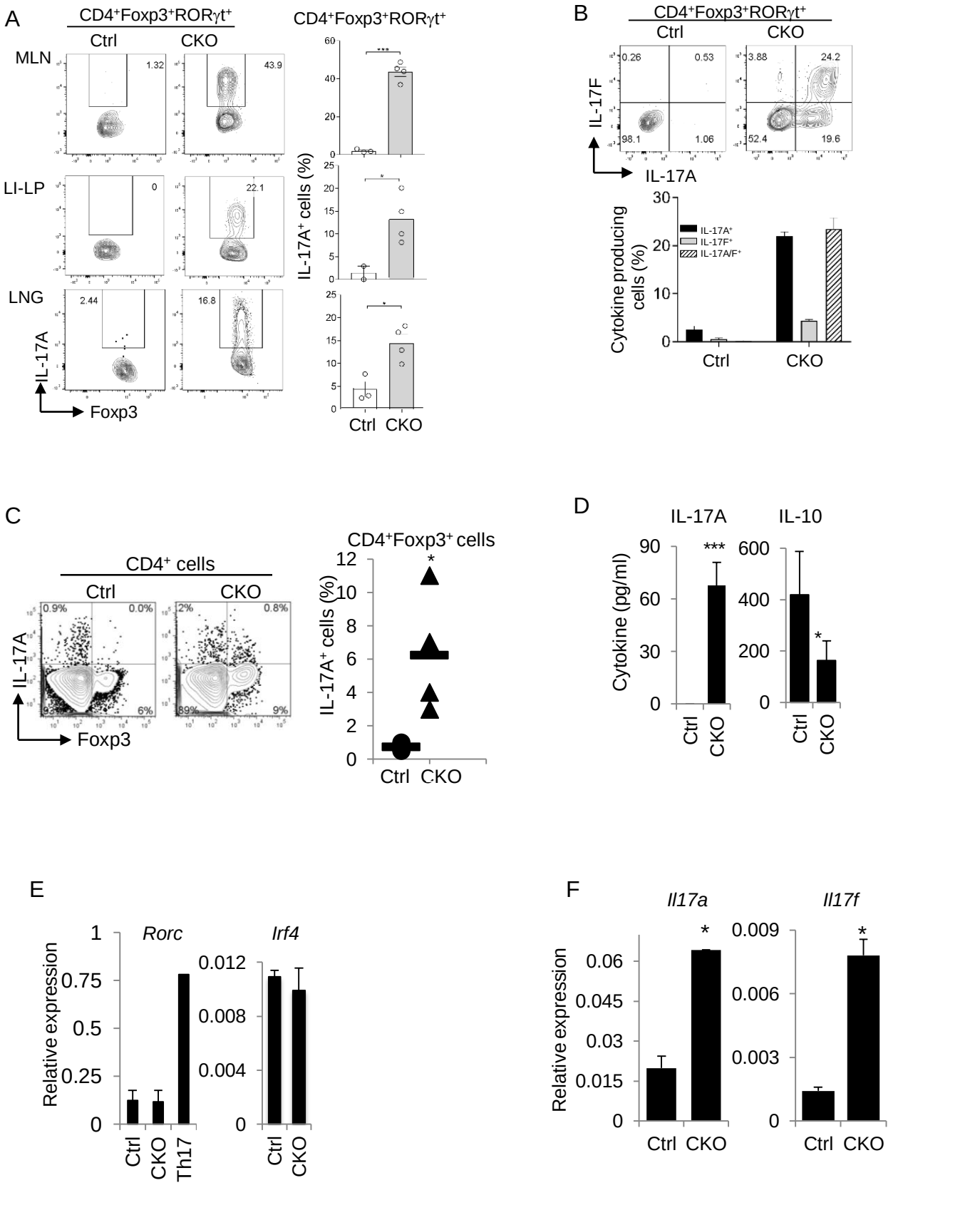

Supplemental Figure 2: Requirement of Blimp-1 to suppress IL-17 expression in Foxp3^{+}RORγt^{+}Treg cells, related to Figure 1. (**A**) Representative Facs plots (left) and cumulative data (graphs, right) showing the frequency of IL-17A^{+} cells in CD4^{+}Foxp3^{+}RORγt^{+} cells from the mesenteric lymph nodes (MLN), colonic intestinal lamina propria (LI-LP) and lungs (LNG) from Ctrl or *Prdm1*$^{F/F}$CD4^{CRE+} (CKO) mice. Cells were stimulated by PMA and ionomycin for 4 h with addition of Brefeldin A for the last 2 h before intracellular cytokine staining. (**B**) Expression of IL-17A and IL-17F in CD4^{+}Foxp3^{+}RORγt^{+} cells from the MLN of Ctrl and *Prdm1*$^{F/F}$CD4^{CRE+}Foxp3^{GFP} (CKO) mice. Cells were stimulated as in (**A**) before staining. (**C**) Expression of IL-17A and Foxp3 protein in cells from the MLN of Ctrl or *Prdm1*$^{F/F}$CD4^{CRE+} (CKO) mice. Cells were stimulated as in (**A**) before staining. (**D**) IL-17A and IL-10 expression (ELISA) in supernatants of CD4^{+}Foxp3^{GFP+} cells sort purified from Ctrl or *Prdm1*$^{F/F}$CD4^{CRE+}Foxp3^{GFP} mice and stimulated with anti-CD3 and CD28 for 18 h. (**E**) *Irf4* and *Rorc* mRNA expression (qRT-PCR, relative to β2microglobulin) in CD4^{+}Foxp3^{GFP+} cells sorted from Ctrl and *Prdm1*$^{F/F}$CD4^{CRE+}Foxp3^{GFP} (CKO) mice. (**F**) *Il17a* and *Il17f* mRNA expression (qRT-PCR) in CD4^{+}Foxp3^{GFP+} cells sorted from SP and MLN from Ctrl and *Prdm1*$^{F/F}$CD4^{CRE+}Foxp3^{GFP} (CKO) mice and stimulated *in vitro* with anti-CD3 and CD28 for 24 h. Data shown is from at least two independent experiments. Bars show average and error bars, SEM (N ≧ 3 mice/group). *p<0.05 and ***p<0.001, unpaired student's t test.

Supplemental Figure 3

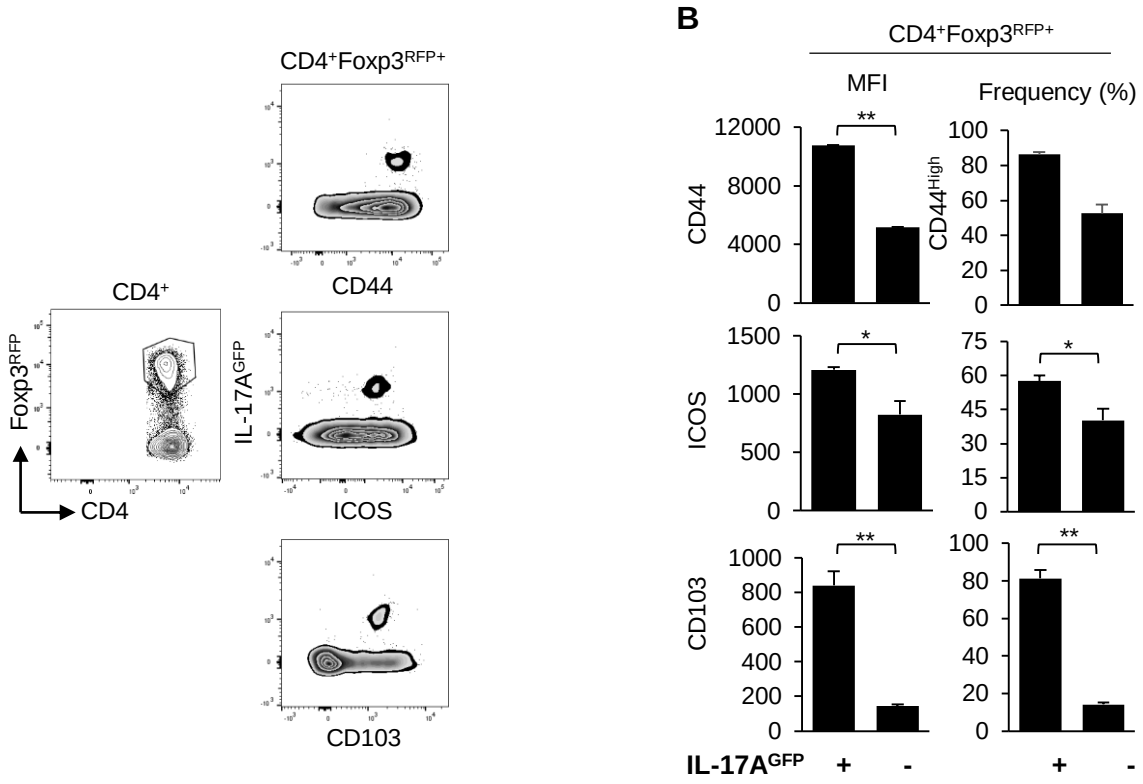

Supplemental Figure 3: Preferential expression of activator molecules by IL-17-producing Blimp-1-deficient RORγt⁺ Treg cells, related to Figure 1. (A) Representative FACS plots of IL-17A^{GFP} and effector molecules (CD44, ICOS and CD103) expression in CD4^{+}Foxp3^{RFP+}Treg cells from the spleen from *Prdm1*$^{F/F}$CD4^{CRE+}Foxp3^{RFP}IL-17A^{GFP} mice. (**B**) Cumulative expression data (MFI and frequency) of same molecules as in A, in IL-17A^{GFP+} and IL-17A^{GFP-} CD4^{+}Foxp3^{RFP+}Treg cells. Bars (**B**) show average and error bars, SEM (N = 3 mice). **p*<0.05 and ***p*<0.01, paired student's *t* test.

Supplemental Figure 4

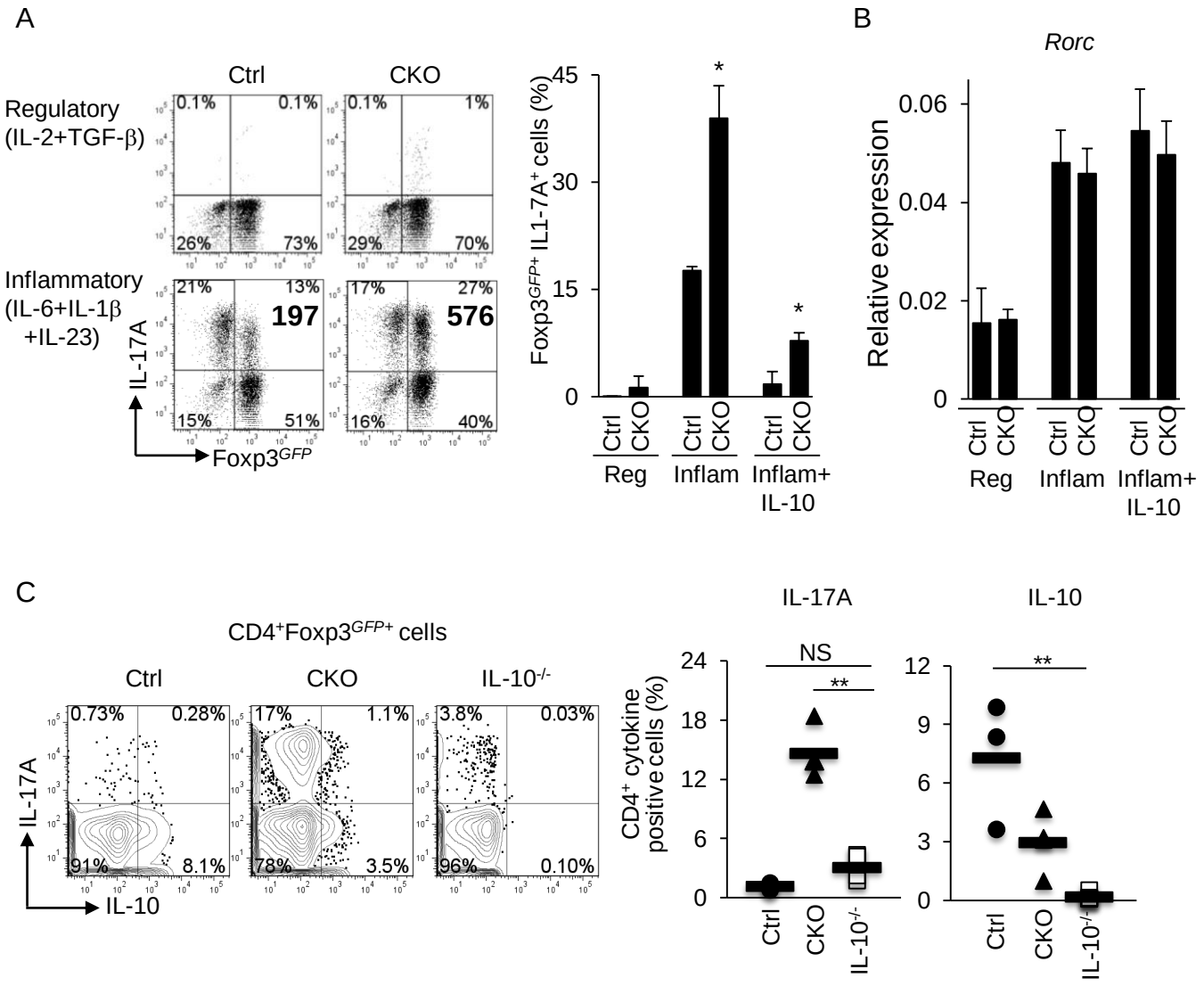

Supplemental Figure 4: Expression of IL-17 by Blimp-1-deficient Foxp3⁺ Treg cells is not secondary to impaired IL-10 expression, related to Figure 1. (**A**) FACS plots (left) showing expression of IL-17A and Foxp3^{GFP} in sorted CD4^{+}Foxp3^{GFP+} cells from *Prdm1*$^{+/+}$CD4^{CRE+} (Ctrl) and *Prdm1*1$^{F/F}$CD4^{CRE+} (CKO) mice. Sorted cells were in the presence of IL-2 and TGF-β, (regulatory conditions; top plots), or IL-6, IL-1b and IL-23 (inflammatory conditions; bottom plots) or inflammatory condition plus rMuIL-10 for 5 days and then re-stimulated for 6 hours (anti-CD3 and CD28). Bar graph (right) shows frequency of IL-17A^{+} cells in CD4^{+}Foxp3^{GFP+} cells. Numbers in bold in FACS plots are MFI of IL-17A staining. (**B**) *Rorc* mRNA expression (qRT-PCR, relative to β2microglobulin) in same cells shown in (**A**). (**C**) FACS plots (left) and scatter plots (right) showing expression of IL-17A and IL-10 in splenic CD4^{+}Foxp3^{GFP+} cells from Blimp1-suffcient (Ctrl), Blimp-1-deficient (CKO) and Blimp-1-sufficient IL-10$^{-/-}$ mice (IL-10$^{-/-}$). Data shown is representative from at least two independent experiments. Bars show average and error bars, SEM (N ≧ 3 mice/group). *p<0.05, **p<0.01, unpaired student's t test (**A** and **B**), one-way ANOVA (**C**).

Supplemental Figure 5

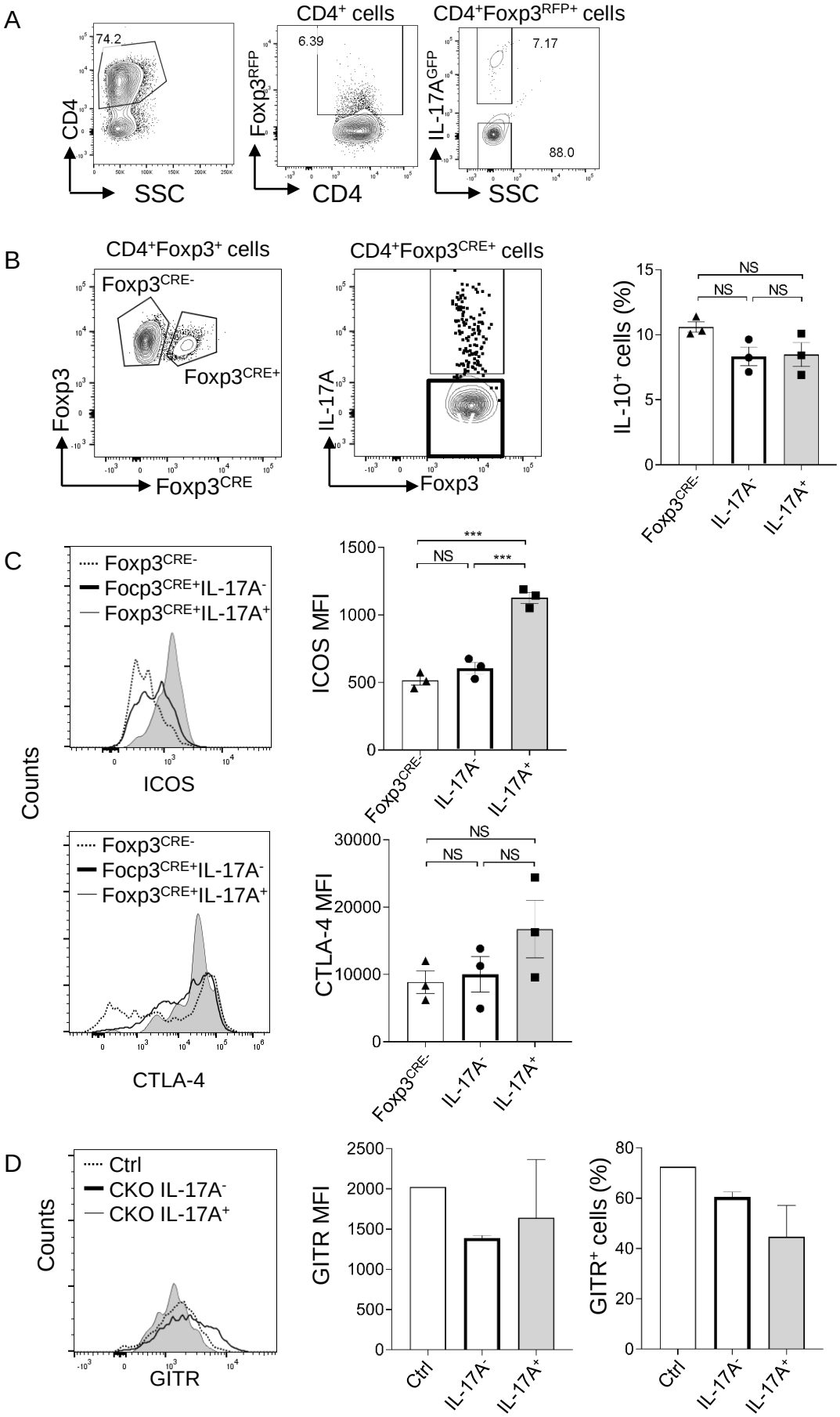

Supplemental Figure 5: Expression of Treg effector molecules does not segregate with IL-17A expression in Blimp-1-deficient Foxp3^{+} Treg cells, related to Figure 4. (**A**) FACS plots showing gating strategy for sorting of IL-17A^{GFP+} and IL-17A^{GFP}CD4^{+}Foxp3^{RFP+} cells from *Prdm1*$^{F/F}$CD4^{CRE+}Foxp3^{RFP}IL-17A^{GFP} mice. (**B**) IL-10 expression in Blimp-1-sufficient (CRE-) and Blimp-1-deficient (CRE+) in IL-17A^{GFP+} and IL-17A^{GFP-} Foxp3^{+}Treg cells from Prdm1$^{F/F}$ Foxp3^{CRE+} female mice. (**C**) Expression (median intensity fluorescence, MFI) of ICOS and CTLA-4 in the same cells shown in (**B**). (**D**) Expression (MFI, left and frequency, right) of GITR in Blimp-1-sufficient, and Blimp-1-deficient Foxp3^{+}IL-17A^{+} and Foxp3^{+}IL-17A^{-} cells from *Prdm1*$^{F/F}$CD4^{CRE+} mice. Bars show average and error bars, SEM (N ≧ 3 mice/group). ***p<0.001, one-way ANOVA (**B** and **C**).

Supplemental Figure 6

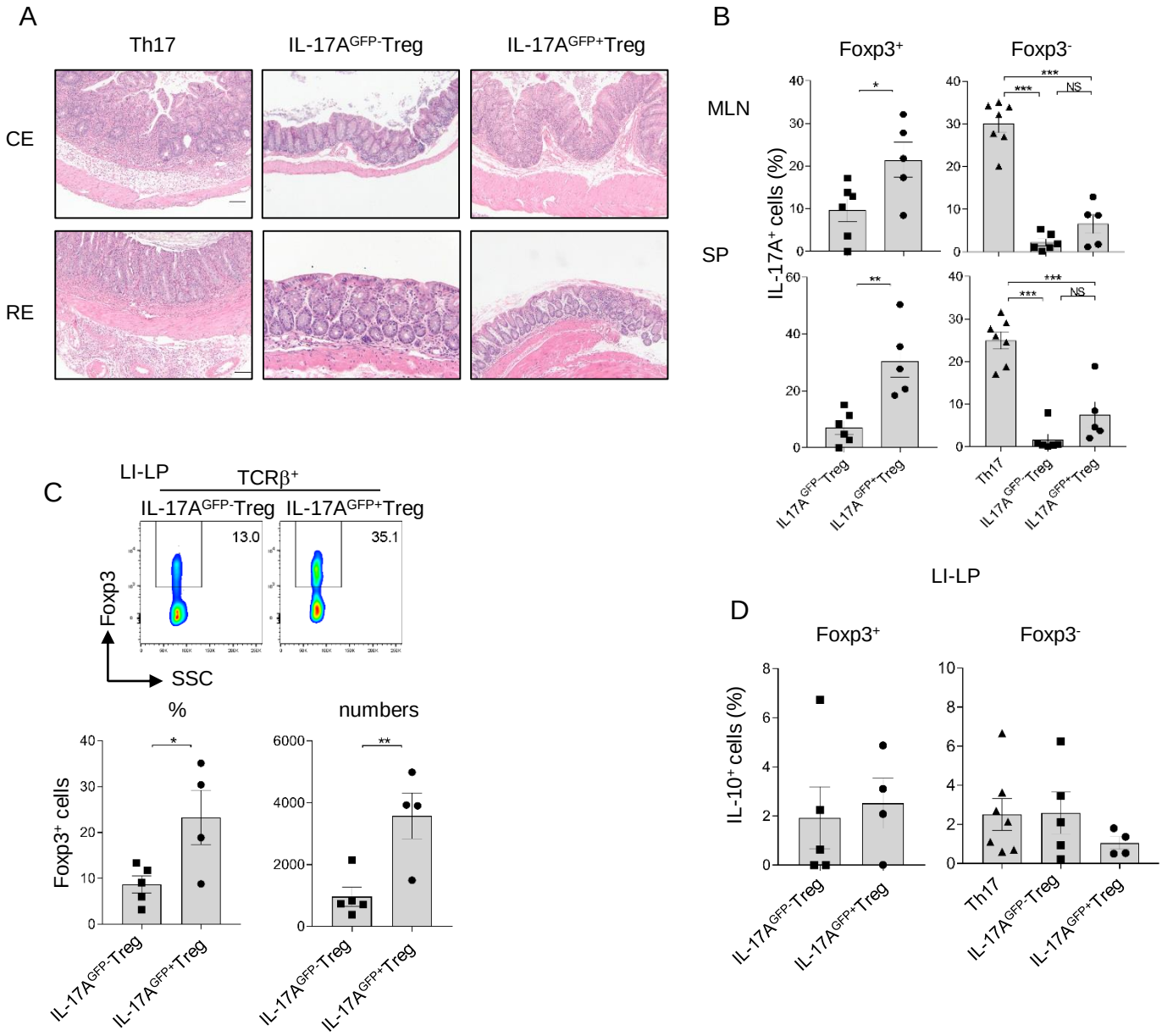

Supplemental figure 6: IL-17-expressing Blimp-1-deficient Foxp3$^+$ cells cause mild intestinal inflammation upon adoptive transfer to RAG1$^{-/-}$ mice, related to Figure 4. (**A**) histological sections (10x magnification, scale bar shown in first figure on the left, indicate 100 μm) of cecum (top) and rectum (bottom) of RAG1$^{-/-}$ mice adoptively transferred with in vitro differentiate wild type Th17 cells (Th17), Blimp-1-deficient IL-17A-producing (IL-17^{GFP+}Treg) or non-producing (IL-17A^{GFP-}Treg) Foxp3$^+$ Treg cells. (**B**) Graphs showing the frequency of IL-17A-producing Foxp3$^+$ (left) and Foxp3$^-$ (right) cells from the MLN (top) and SP (bottom) recovered from recipient mice 4 weeks post transfer. (**C**) FACS plots (top) and bar graphs (bottom) showing frequency (left graph) and number (right graph) of Foxp3 expression in adoptively transferred cells recovered from the intestinal lamina propria (LI-LP) from recipient mice 4 weeks post transfer. (**D**) Expression of IL-10 in Foxp3$^+$ (left) and Foxp3$^-$(right) cells from same mice as in A-C. Data shown is from three different experiments. Error bars, SEM (N=5-7mice/ group). *p<0.05, **p<0.01 and ***p<0.001, unpaired student t test (**C** and **D**) and one-way ANOVA (**B** and **D**).